

CHAPTER 4

NINE LEVEL INVERTER WITH CURRENT INJECTION CIRCUIT USING PASSIVE NETWORK

This section explains a soft-switched, single-stage converter for medium to high voltage high power factor ASD with MLI. No separate switches or converter is needed for line current shaping and for driving the motor run like conventional methods. The high-frequency current is injected from Diode Clamped Multilevel Inverter (DCMLI) to the three-phase rectifier hence, producing a high-frequency modulation of the rectifier input voltages. This results in inherent high PF operation due to the Continuous Conduction Mode (CCM) of operation of input source inductors. In this way, the need of active front-end rectifier with insulated gate bipolar transistors (IGBTs) is eliminated. The topology is described by low Electro Magnetic Interference (EMI) conduction, low THD and low switching loss owing to soft switching.

The significant advantages of the proposed schemes are: the switching stresses are decreased to half of the conventional methods because shunt capacitor voltage is divided by two switches, and it does not require additional active components for current injection, and that makes it suitable for high-voltage drive applications. The work proposes a compensation algorithm using passive current injection associated with the ASD to compensate current harmonics due to non-linear loads. Institute of Electrical and Electronics Engineers (IEEE) and Geneva-based International Electro technical Commission (IEC) have proposed various standards for power quality. Table 4.1 lists various power quality standards as recommended by IEC and IEEE.

Table 4.1 Power quality standards of IEC and IEEE

Phenomena	Standards
Classification of power quality	IEC 61000-2-5:1995[2] IEC 61000-2-1:1990[3] IEEE 1159:1995[4]
Harmonics	IEC 61000-2-1:1990[3] IEEE 519:1992[7] IEC 61000-4-7:1991[8]
Voltage sag/swell and interruptions	IEC 61000-2-1:1990[3] IEEE 1159:1995[4]
Transients	IEC 61000-2-1:1990[3] IEEE c62.41:(1991)[5] IEEE 1159:1995[4] IEC 816:1984[6]
Voltage Flicker	IEC 61000-4-15:1997[9]

Table 4.2 and Table 4.3 show the voltage harmonic limits for different voltage levels and current harmonic limits for various types of loads.

Table 4.2 IEEE 519: Voltage Distortion Limits

Bus Voltage at PCC	Individual V(p. u)	Voltage THD (percent)
Above 161kV	1.0	1.5
Between 161 kV and 69kV	1.5	2.5
Less than 69kV	3.0	5.0

Table 4.3 Equipment Harmonic Current Limits

Equipment	Limit(% THD-Current)
All fluorescent lighting, including compact fluorescent	30
High-efficiency single phase heat pumps and air conditioners	25
All lighting, motor drives, power supplies and other equipment sharing a common electrical bus or panel with sensitive electronic loads	15
Switching power supplies, computers, electric vehicles	30
All other equipment	30

4.1 ASDWithCurrent Injection Using Passive Network

The proposed three-phase HF current injection topology is depicted in Figure.4.1. It consists of line source inductors ($L_{SR}-L_{SB}$), a three-phase diode bridge rectifier (D_1-D_6) and HF current injection circuit. The HF current injection circuit comprises of three-phase DCMLI, DC blocking capacitors (C_1-C_3) and high-frequency inductors (L_1-L_3). In the input side of the three-phase rectifier, inductors are connected.

The output DC voltage, V_{dc} of the rectifier performs as the input to the inverter through four split capacitors ($C_{dc1}-C_{dc4}$). Each leg of the DCMLI consists of six clamping diodes and eight active switches (S_1-S_8). One phase-leg of a three-level DCMLI comprises of four IGBTs and two clamping diodes. The other two phase-legs would be joined across the same DC bus,

and the clamping diodes joined to the same midpoint of the DC capacitor. Nine level diode-clamped inverter operation have been explained in chapter 3.2.

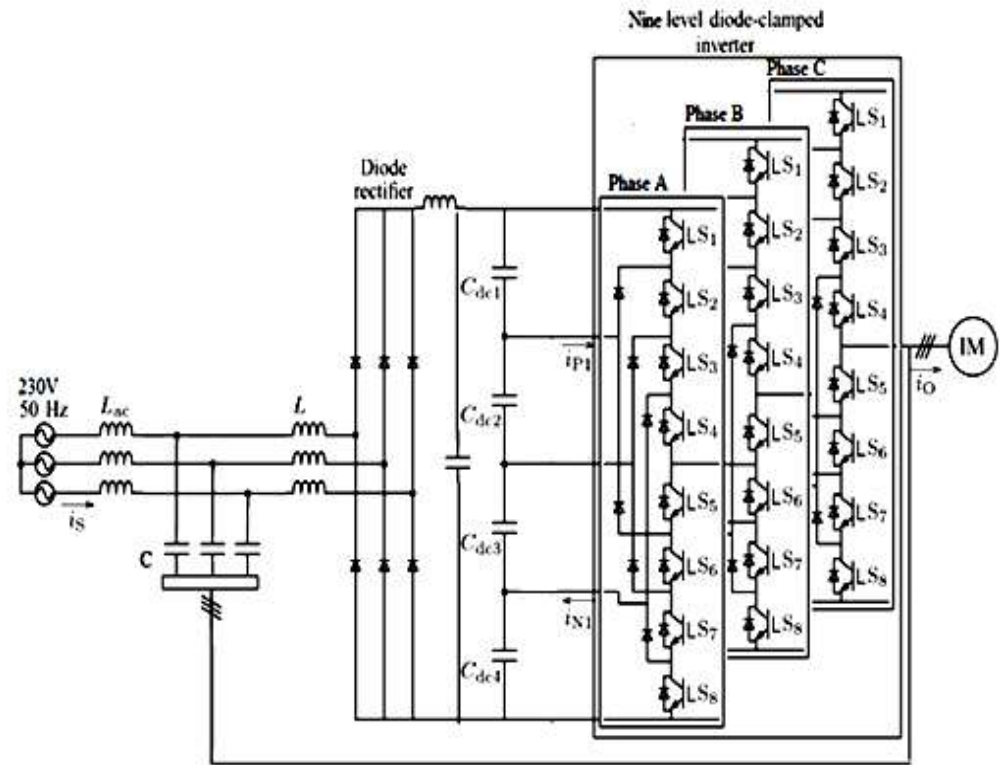


Figure 4.1. Nine level inverter with passive current injection circuit

If the AC voltage pulse width is of duration “ σ ” per half-cycle, then the fundamental RMS voltage is given by:

$$V_1 = \frac{2\sqrt{2}}{\pi} \left(\frac{V_{DC}}{2} \right) \sin \frac{\sigma}{2} = \frac{2\sqrt{2}}{\pi} \left(\frac{V_{DC}}{2} \right) \cos \alpha \quad (4.1)$$

Where

$$\sigma = \pi - 2\alpha$$

V_{dc} = DC link voltage.

4.2 Principle of operation of Passive Compensation

In the converter, inductances (L_1 - L_3) and feedback capacitors (C_1 - C_3) are designed for high-frequency operation. Therefore, the feedback capacitor offers very high impedance to supply voltage. The voltage across the capacitor C_1 (v_{C1}) has the modulation of supply frequency of 50 Hz. Therefore, at any instant the voltage across the C_1 is equal to the supply voltage, v_R . As the capacitor carries HF current, the v_{C1} has HF voltage ripples superimposed on the power frequency component. This capacitor also serves the purpose of dc blocking to the injected current. The devices are switched at high frequency f_s . During a particular switching interval, k , when lower switches S_{13} and S_{14} are off and upper switches S_{11} and S_{12} are on, the voltage across L_1 , v_{L1} is same as the input phase voltage v_R . The current i_{L1} , through the inductor L_1 increases linearly from 0 to its maximum value I_{L1p} (Figure.4.2) at the rate proportional to the instantaneous value of the supply phase voltage v_R . The other inductors current also increase at the rate proportional to the instantaneous values of their corresponding phase voltages.

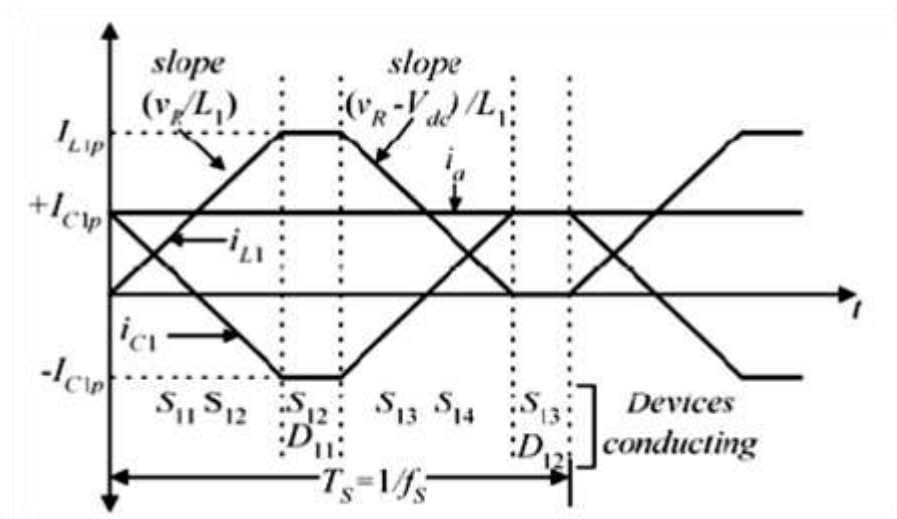


Figure 4.2. Idealized inductor, capacitor and supply currents

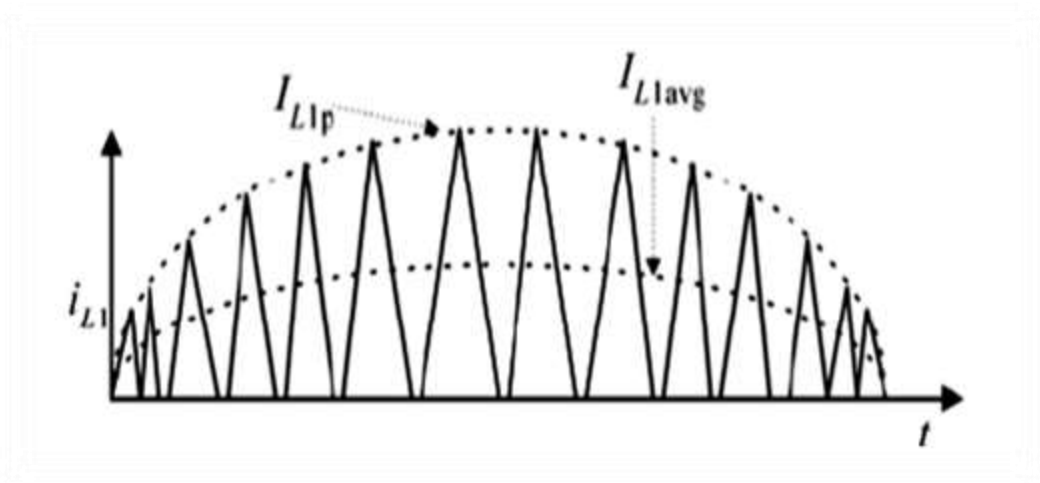


Figure 4.3 Inductor current overlap

At the same time, the capacitor current, i_{C1} diminishes from its positive maximum $+I_{C1p}$ to negative maximum $-I_{C1p}$ through 0. Because of high-frequency switching, the supply current i_R is the sum of average values of i_{L1} and i_{C1} . So, input supply current is given by:

$$i_R = I_{L1avg} + I_{C1avg} \quad (4.2)$$

Where,

I_{L1avg} is average value of inductor

I_{C1avg} is average value of capacitor current

During the interval when upper switches (S_{11} and S_{12}) are on:

$$I_{L1avg} = \left(\frac{I_{L1p}}{2}\right), I_{C1avg} = 0 \quad (4.3)$$

When switches, S_{12} and S_{13} are on (S_{11} and S_{14} off), the voltage across L_1 is $(V_{dc}/2) - v_R$. The current i_{L1} remains constant at I_{L1p} and capacitor current is $-I_{C1p}$. During this interval, as clamping diode D_{11} conducts and i_{L1} remains constant, the voltage across L_1 is zero. When lower switches, S_{13} and S_{14} are on,

the voltage across L_1 is $(v_R - V_{dc})$. The i_{L1} diminished from its maximum value I_{L1p} to zero and remains zero till the next cycle begins. The i_{C1} ramps up to its peak value $+I_{C1p}$ from $-I_{C1p}$ and remains at $+I_{C1p}$ till the next cycle begins. The maximum current value, I_{L1p} in a particular switching cycle, varies with the value of input voltage in that cycle. The values of input voltage, during different switching cycles, vary sinusoidally. Hence, the peak values, I_{L1p} also varies sinusoidally in the envelope defined by the supply phase voltage as shown in Figure. 4.3. The supply current, i_R is the addition of average values of i_{C1} and i_{L1} . In addition to, the average value of i_{C1} over a switching cycle is zero. Therefore, i_R is equal to the I_{L1avg} . Since, each time inductor current pulses begin at zero (discontinuous conduction), the i_R and I_{L1avg} also vary sinusoidally in phase with the supply voltage. The same action takes place in other phases and in the negative half-cycle also. Therefore, the overall power factor is very close to unity. During the complete cycle of the supply voltage, the HF switching of inductor forces diodes of the three-phase rectifier to turn on and off at the switching frequency. When none of the diodes is conducting, the supply current flows through the capacitor C_1 , the switch S_{13} and the clamping diode D_{12} . Thus, it maintains the continuous current through the source inductor L_{SR} . In continuous conduction mode (CCM) means the current in the energy transfer inductor never goes to zero between switching cycles. Hence, the discontinuity in the supply current, which is mainly responsible for deteriorating the quality of the supply current, is removed which results in CCM operation of source inductor. As a result, the operation of source inductors in CCM leads to improvement in input power factor and inherent active wave shaping of input current.

4.3 Performance Analysis

To simplify the analysis, the following assumptions are made:

- Input three-phase supply is balanced and purely sinusoidal;
- The switching frequency is far greater than the power line frequency ($f_s \gg f$);
- The resistance of the inductors is adequately small to be neglected;
- All the switches are ideal.

The three-phase voltages are given by:

$$v_R = V_p \sin(\omega t), v_Y = V_p \sin(\omega t - \frac{2\pi}{3}), v_B = V_p \sin(\omega t + \frac{2\pi}{3}) \quad (4.4)$$

4.3.1 Input Supply Current, i_R

Since the switching frequency is very high, the AC line current in a switching period, as stated earlier, is the sum of average values of i_{L1} and i_{C1} .

Therefore,

$$i_R = i_{L1(avg)} + i_{C1(avg)} \quad (4.5)$$

$$i_{L1(avg)} = \frac{1}{T_s} \left[\int_0^\sigma \left(\frac{I_{L1p}}{\sigma} t \right) dt + \int_\sigma^{\sigma+2\alpha} I_{L1p} dt + \int_{\sigma+2\sigma}^{2\sigma+2\alpha} \frac{I_{L1p}}{\sigma} (-t + 2\sigma + 2\alpha) dt + \int_{2\sigma+2\alpha}^{2\sigma+4\alpha} I_{L1p} dt = \frac{I_{L1p}}{2} \right] \quad (4.6)$$

From the above equation, the average current is given by

$$i_{L1(avg)} = \frac{v_R}{2L_1} \left(\frac{\sigma}{\omega_s} \right) \quad (4.7)$$

If T_s is the switching period of the DCMLI and V_p is the peak value of

the supply phase voltage, then equation (4.7) can be given as

$$i_{L1(avg)} = \frac{\sigma T_S}{4\pi L_1} (V_P \sin(\omega t)) \quad (4.8)$$

The average value of a current through capacitor i_{C1} is zero.

Therefore, equation (4.2) and (4.8) lead to supply current as

$$i_R = \frac{\sigma T_S}{4\pi L_1} (V_P \sin(\omega t)) = K V_P \sin(\omega t) \quad (4.9)$$

Where K is a constant, having value

$$K = \frac{\sigma T_S}{4\pi L_1}$$

The above equation clearly indicates that the input supply current i_R is always in phase with supply voltage v_R . The phase angle difference of i_R and v_R is zero. Hence, the designed converter operates at unity power factor. Detailed diagrams are shown in Chapter 5.

4.3.2 Input power and current

Input power is given by

$$P = 3 \left[\frac{1}{\pi} \int_0^\pi v_R i_R d\omega t \right] \quad (4.10)$$

Where,

v_R is the supply phase voltage

i_R is the supply phase current.

From equation 4.4 and 4.9,

$$P = 3 \frac{1}{\pi} \int_0^\pi v_p \sin \omega t \cdot \frac{\sigma T_S}{4\pi L_1} v_p \sin \omega t d\omega t = \frac{3v_p^2 \sigma T_S}{8\pi L_1} \quad (4.11)$$

Input rms current can be given as

$$I_{Rrms} = \sqrt{\frac{1}{\pi} \int_0^{\pi} \left(\frac{\sigma T_S}{4\pi L_1} V_P \right)^2 \sin^2 \omega t d\omega t} = \frac{\sigma T_S V_P}{4\sqrt{2}\pi L_1} \quad (4.12)$$

4.3.3 Design of inductor, L_1

Three phase power is given by

$$P = 3V_{Rrms}I_{Rrms} \quad (4.13)$$

$$P = 3 \frac{V_p}{\sqrt{2}} \frac{\sigma T_S V_p}{4\sqrt{2}\pi L_1} \quad (4.14)$$

From equation 4. 14, the value of the inductor L_1

$$L_1 = \frac{3v_p 2\sigma T_S}{8\pi P_o} \quad (4.15)$$

If η is efficiency and P_O is output power of the converter then

$$L_1 = \frac{3v_p 2\sigma T_S \eta}{8\pi P} \quad (4.16)$$

4.3.4 Design of capacitor, C_1

The RMS value of the current through the capacitor, C_1 is given as

$$I_{Crms} = \frac{I_p}{\sqrt{3}} \sqrt{\frac{3\pi-2\sigma}{\pi}} \quad (4.17)$$

Energy stored in the capacitor is given by

$$\frac{1}{2} C_1 V_{rms}^2 = V_{rms} I_{rms} T_S \quad (4.18)$$

$$C_1 = \frac{2 \left[\frac{I_p}{\sqrt{3}} \left(\sqrt{\frac{3\pi-2\sigma}{\pi}} \right) \right] T_S}{V_{Rrms}}$$

$$C_1 = \frac{4\sqrt{2}P_0 \left(\sqrt{\frac{3\pi-2\sigma}{\pi}} \right)}{3V_P 2f_s \eta} \quad (4.19)$$

Where,

f_s is switching frequency

p_o is the output power

η is the converter frequency.

4.4 Design of the Current Injection Circuit

4.4.1 Specifications of the converter

Rated ac input voltage per phase $V_R=230V$;

Input supply frequency, $f=50Hz$;

DC bus voltage, $V_0=540 V$;

Rated output of the converter, $P_0=2.2kW$;

Switching frequency, $f_s=50kHz$.

4.4.2 Calculations of Inductor and Capacitor

a. Feedback inductor (L_1-L_3)

Using Equation.4.16 with output power, $P_0=2.2kW$, $\sigma=150^\circ$ and assumed efficiency of the converter as 92%, the value of the feedback inductor

is estimated to $L_1 = \frac{3v_p 2\sigma T_S}{8\pi P_0}$

b. Feedback capacitor(C_1-C_3)

Feedback capacitor can be evaluated by using Equation (4.19)

$$C_1 = \frac{4\sqrt{2}P_0 \left(\sqrt{\frac{3\pi-2\sigma}{\pi}} \right)}{3V_P 2f_s \eta} \quad (4.20)$$

Hence, $C_1=C_2=C_3=1\mu F$ (poly propylene capacitor) is chosen

4.4.3 Calculations of Filter Components

The output filter is connected between an induction motor and multilevel inverter. The maximum resonance frequency of the filter is chosen to be the half of the switching frequency. The design is carried out: $f_c = \frac{1}{2\pi\sqrt{LC}}$,

Where, f_c is the cutoff frequency $f_c = 25$ kHz. The filter L and C components are found to be $L = 1$ mH and $C = 40$ nF due to high frequency, switching the filter components size and cost are greatly reduced.

4.5 Results And Discussion

Three phase Nine level diode clamped multilevel inverter fed induction motor with front end rectifier and passive network compensation is simulated with PSIM software and simulation parameters tabulated in Table 4.4. The sub-block consists of one arm of the nine levels DCMLI, where all switches are connected in series with the parallel combination of clamping diodes. The clamping diodes are connected with capacitors, as shown in Figure 4.4. Switching states of a positive arm are complementary to the negative arm. So the pulses generated for a positive arm are inverted and given to the negative arm. Three phase Nine level diode clamped multilevel inverter fed induction motor with passive current injection is analysed. The passive current injection network is made up of resonating components. The absence of active switches is the advantage of this network. It makes the system simple and cost effective.

Table 4.4 Induction Motor Simulation Parameters

Parameters	Values
R_s (stator)	1.405
L_s (stator)	0.005839
R_r (rotor)	1.395
L_r (rotor)	0.005839
L_m (magnetizing)	0.1722
No of poles	4

Figure. 4.5 demonstrate the injected current waveform to make the compensation on the distorted input current of diode rectifier. The passive compensation network is added to inject the harmonic component in the diode rectifier input current. As a result, the distortion available in the input current is decreased.

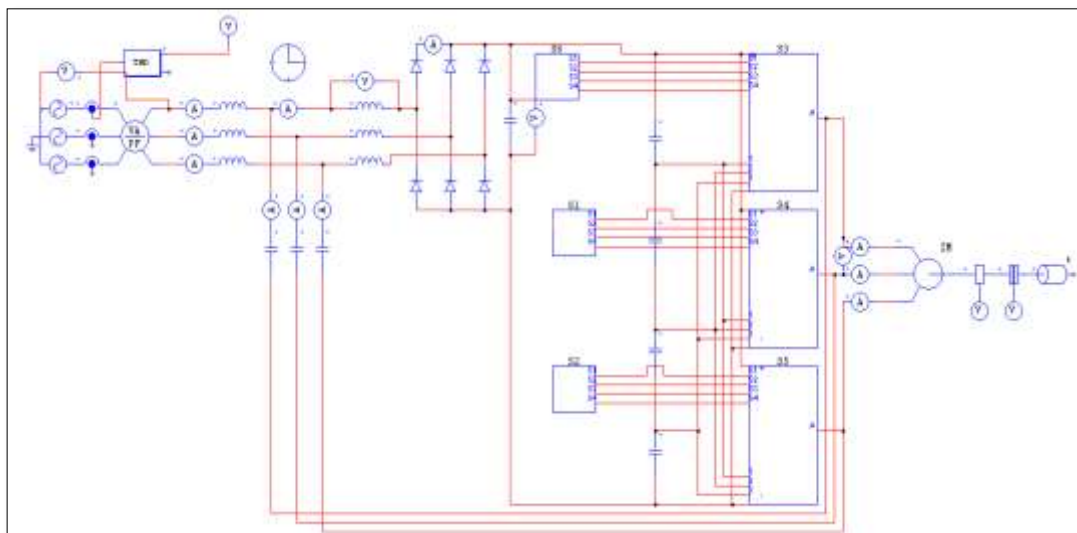


Figure.4.4 PSIM model of nine level diode clamped multilevel inverter fed induction motor with passive current injection circuit

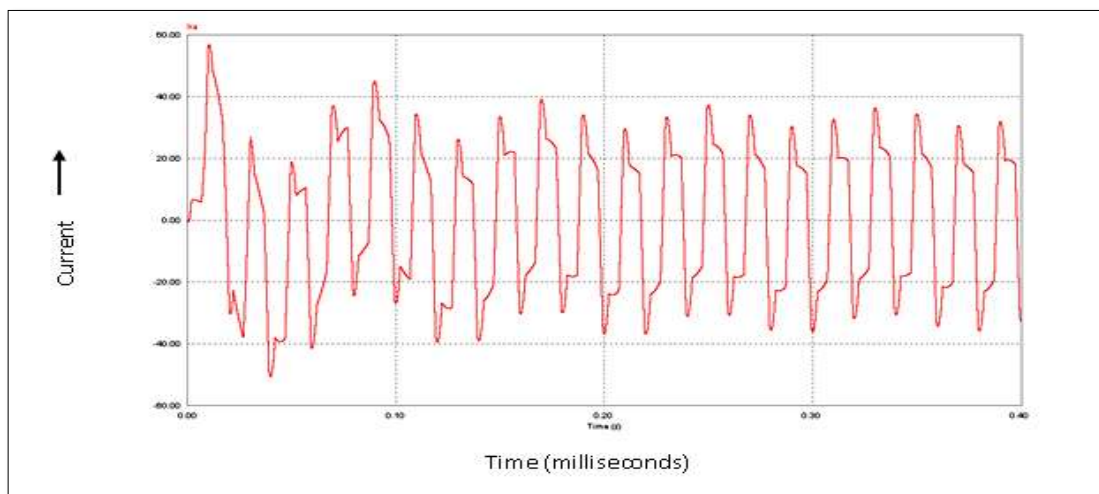


Figure.4.5 Injected current Ira: 20A/div Time: 0.10msec/div

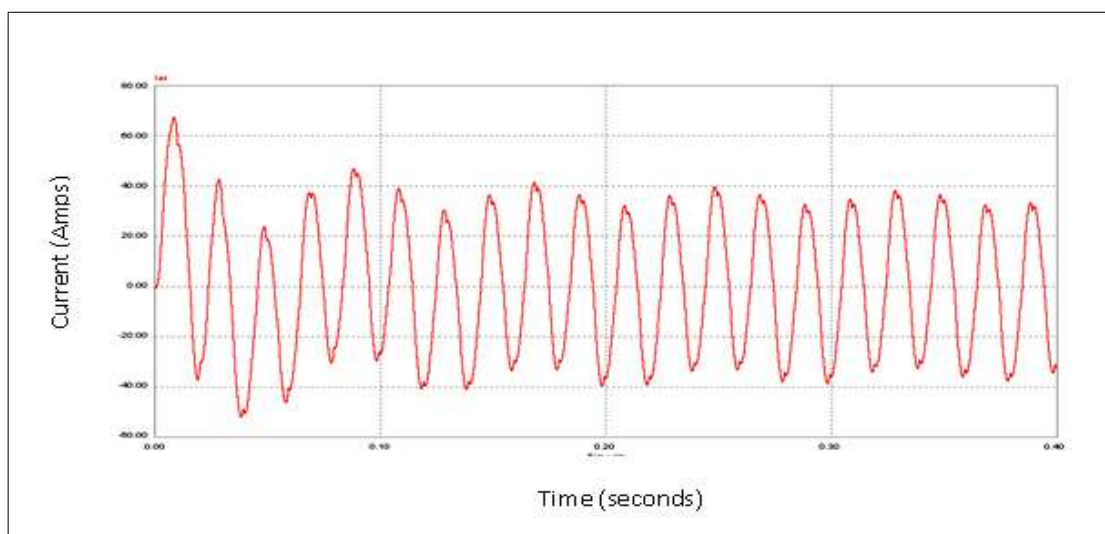


Figure.4.6 Source current with compensation 20A/div. Time: 0.1s/div

The Figure. 4.6 demonstrates the per phase compensated input current of six-pulse diode rectifier. It is nearly sinusoidal when compared with an uncompensated waveform as shown in the Figure. 3.12.

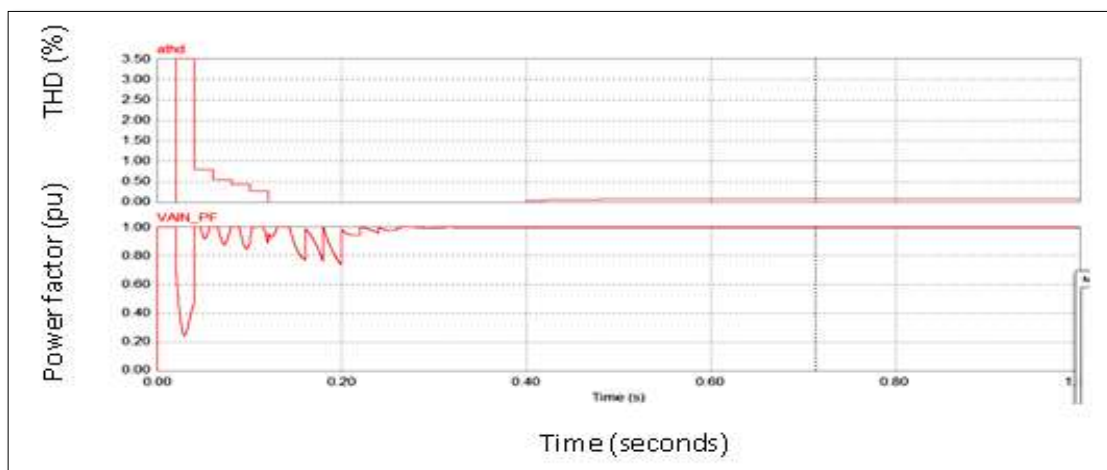


Figure.4.7 THD and PF; a thd(THD): 0.5pu/div.

$V_{A_IN_PF}$ (PF):0.2pu/div. Time: 0.2s/div

The PF and THD of supply current obtained from simulation are shown in Figure4.7. The Total harmonic distortion of the compensated supply current is 7.72 % and power factor is 0.99. This indicates that performance is improved when compared with existing results illustrated in the Figure. 3.14

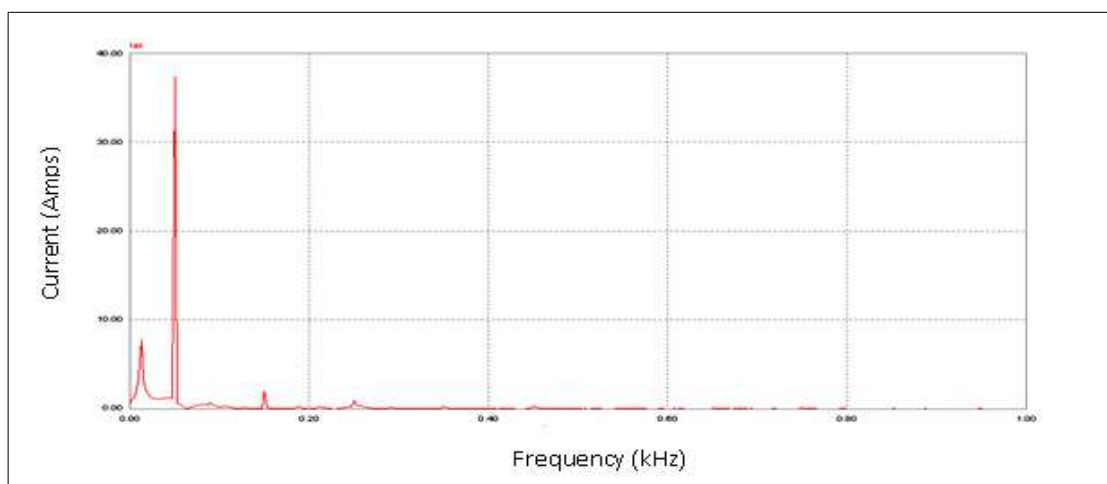


Figure 4.8 FFT spectrum 10A/div. Frequency: 0.2kHz/div

The Figure.4.8 displays the FFT spectrum of the supply current is obtained from simulation. It explains the order of harmonics. Waveform clearly shows the absence of harmonic current.

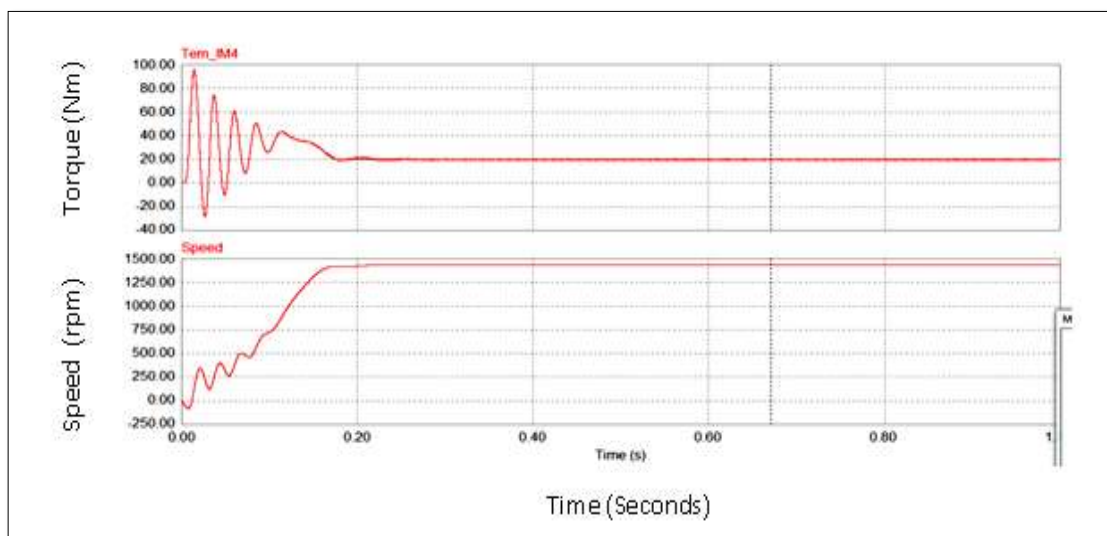


Figure 4.9 Torque and Speed at full load (Simulation)

Tem_IM4(Torque): 20Nm/div. Speed: 250rpm/div

The mechanical characteristics of torque and speed of an induction motor obtained from simulation are shown in Figure. 4.9. The inverter fed induction motor has smooth speed – torque characteristics. The speed of an induction motor is around 1350 rpm, and its torque developed in the motor is 20 Nm. The torque pulsation is almost zero. The settling time of the given motor drive is about 0.18 Sec.

4.6 Summary

An ASD with high input PF and improved harmonic performance has been analyzed. The PF of the three-phase AC input line current is enhanced by injecting the HF current. In this approach, any additional active components are not needed for HF current injection. Due to the high frequency current injection, capacitor C_f and inductors L_f value is decreased. Various results are obtained. The obtained value of PF and THD are 0.99 (lagging) and 7.72%, respectively, which is more desirable. The simulation results of multilevel inverter show improved the harmonic profile of output voltage waveform. It is about 9%. The high-quality voltage used to drive the induction motor. It

causes good torque-speed characteristics of the induction motor. Chapter 5 explains the harmonic reduction in the supply current by introducing an active current injection technique.